A. J. McMichael. 1991. Human immunodeficiency virus genetic variation that can escape cytotoxic T cell recognition. Nature **354:**453–459.

37. **Sauce, D., J. R. Almeida, M. Larsen, L. Haro, B. Autran, G. J. Freeman, and V. Appay.** 2007. PD-1 expression on human CD8 T cells depends on both state of differentiation and activation status. AIDS **21:**2005–2013.
38. **Sharpe, A. H., and G. J. Freeman.** 2002. The B7-CD28 superfamily. Nat. Rev. Immunol. **2:**116–126.
39. **Streeck, H., Z. L. Brumme, M. Anastario, K. W. Cohen, J. S. Jolin, A. Meier, C. J. Brumme, E. S. Rosenberg, G. Alter, T. M. Allen, B. D. Walker, and M. Altfeld.** 2008. Antigen load and viral sequence diversification determine the functional profile of HIV-1-specific CD8+ T cells. PLoS Med. **5:**e100.
40. **Stuber, G., S. Modrow, P. Hoglund, L. Franksson, J. Elvin, H. Wolf, K. Karre, and G. Klein.** 1992. Assessment of major histocompatibility complex class I interaction with Epstein-Barr virus and human immunodeficiency virus peptides by evaluation of membrane H-2 and HLA in peptide loading-deficient cells. Eur. J. Immunol. **22:**2697–2703.
41. **Tanabe, M., M. Sekimata, S. Ferrone, and M. Takiguchi.** 1992. Structural and functional analysis of monomorphic determinants recognized by monoclonal antibodies reacting with the HLA class I alpha 3 domain. J. Immunol. **148:**3202–3209.
42. **Tomiyama, H., H. Akari, A. Adachi, and M. Takiguchi.** 2002. Different effects of Nef-mediated HLA class I down-regulation on human immunodeficiency virus type 1-specific $CD8^+$ T-cell cytolytic activity and cytokine production. J. Virol. **76:**7535–7543.
43. **Tomiyama, H., M. Fujiwara, S. Oka, and M. Takiguchi.** 2005. Epitope-dependent effect of Nef-mediated HLA class I down-regulation on ability of HIV-1-specific CTLs to suppress HIV-1 replication. J. Immunol. **174:**36–40.
44. **Trautmann, L., L. Janbazian, N. Chomont, E. A. Said, S. Gimmig, B. Bessette, M. R. Boulassel, E. Delwart, H. Sepulveda, R. S. Balderas, J. Routy, E. K. Haddad, and R. Sekaly.** 2006. Upregulation of PD-1 expression on HIV-specific $CD8^+$ T cells leads to reversible immune dysfunction. Nat. Med. **12:**1198–1202.
45. **Yang, O. O., P. T. Nguyen, S. A. Kalams, T. Dorfman, H. G. Gottlinger, S. Stewart, I. S. Chen, S. Threlkeld, and B. D. Walker.** 2002. Nef-mediated resistance of human immunodeficiency virus type 1 to antiviral cytotoxic T lymphocytes. J. Virol. **76:**1626–1631.
46. **Yokomaku, Y., H. Miura, H. Tomiyama, A. Kawana-Tachikawa, M. Takiguchi, A. Kojima, Y. Nagai, A. Iwamoto, Z. Matsuda, and K. Ariyoshi.** 2004. Impaired processing and presentation of cytotoxic-T-lymphocyte (CTL) epitopes are major escape mechanisms from CTL immune pressure in human immunodeficiency virus type 1 infection. J. Virol. **78:**1324–1332.
47. **Zhang, J. Y., Z. Zhang, X. Wang, J. L. Fu, J. Yao, Y. Jiao, L. Chen, H. Zhang, J. Wei, L. Jin, M. Shi, G. F. Gao, H. Wu, and F. S. Wang.** 2007. PD-1 up-regulation is correlated with HIV-specific memory CD8+ T-cell exhaustion in typical progressors but not in long-term nonprogressors. Blood **109:** 4671–4678.

the FEBS Journal

MINIREVIEW

Protein–protein interactions and selection: generation of molecule-binding proteins on the basis of tertiary structural information

Mitsuo Umetsu[1,2], Takeshi Nakanishi[3], Ryutaro Asano[1], Takamitsu Hattori[1] and Izumi Kumagai[1]

1 Department of Biomolecular Engineering, Graduate School of Engineering, Tohoku University, Sendai, Japan
2 Center for Interdisciplinary Research, Tohoku University, Sendai, Japan
3 Department of Applied Chemistry and Bioengineering, Graduate School of Engineering, Osaka City University, Japan

Keywords
library design; peptide grafting; protein structure; scaffold protein

Correspondence
M. Umetsu, Department of Biomolecular Engineering, Graduate School of Engineering, Tohoku University, Aoba 6-6-11, Aramaki, Aoba-ku, Sendai 980-8579, Japan
Fax: +81 22 795 7276
Tel: +81 22 795 7276
E-mail: mitsuo@kuma.che.tohoku.ac.jp

(Received 29 October 2009, revised 5 February 2010, accepted 24 February 2010)

doi:10.1111/j.1742-4658.2010.07627.x

Antibodies and their fragments are attractive binding proteins because their high binding strength is generated by several hypervariable loop regions, and because high-quality libraries can be prepared from the vast gene clusters expressed by mammalian lymphocytes. Recent explorations of new genome sequences and protein structures have revealed various small, nonantibody scaffold proteins. Accurate structural descriptions of protein–protein interactions based on X-ray and NMR analyses allow us to generate binding proteins by using grafting and library techniques. Here, we review approaches for generating binding proteins from small scaffold proteins on the basis of tertiary structural information. Identification of binding sites from visualized tertiary structures supports the transfer of function by peptide grafting. The local library approach is advantageous as a go-between technique for grafted foreign peptide sequences and small scaffold proteins. The identification of binding sites also supports the construction of efficient libraries with a low probability of denatured variants, and, in combination with the design for library diversity, opens the way to increasing library density and randomized sequence lengths without decreasing density. Detailed tertiary structural analyses of protein–protein complexes allow accurate description of epitope locations to enable the design of and screening for multispecific, high-affinity proteins recognizing multiple epitopes in target molecules.

Introduction

Antibodies are naturally occurring recognition molecules in the immune system, with high binding affinity and specificity. The strong molecular recognition of antibodies plays important roles in the immune system, and it has been applied in therapeutic fields and the detection of disease-associated marker proteins. Various therapeutic and probe antibodies that target biomolecules in living organisms have been selected from the vast gene cluster for antibodies in mammalian lymphocytes by means of hybridoma and *in vitro* selection technologies [1]. This gene cluster can also supply antibodies with affinity for nonbiological materials [2,3]. The advantage of utilizing antibodies to generate molecules with affinity for a target molecule is the ability to

Abbreviations
^{10}FN3, 10th fibronectin type III domain; CDR, complementarity-determining region; CRAb, chelating recombinant antibody; DARPin, designed ankyrin repeat protein; Fv, fragment of the variable region; NCS, neocarzinostatin; scFv, single-chain fragment of the variable region; TPO, thrombopoietin; VEGF, vascular endothelial growth factor; VHH, variable heavy chain of a heavy-chain camel antibody.

prepare the vast cluster of genes encoding scaffold proteins from lymphocytes; consequently, antibodies have been widely used in medical chemistry [4], imaging [5], and proteomics [6,7].

The presence of the vast gene cluster enables us to obtain valuable binding proteins using selection methodology, and recent structural visualization of candidate proteins by X-ray or NMR structural analyses and the construction of artificial libraries allow constructive selection and functionalization not only of antibody fragments, but also of small, nonantibody proteins (Fig. 1). Accurate structural descriptions of protein–protein interaction provide support for strategies to replace binding site sequences between proteins and library construction in specific areas to increase the density of libraries.

This minireview series describes the methodology for elucidating protein–protein interactions and selecting specific binders to novel target proteins, and the first and second minireviews focus on the detection of protein–protein interactions [8,9]. In this third minireview, we focus on the molecular evolutional methodology for generating and screening binding proteins on the basis of tertiary structures visualized by X-ray and NMR analyses. We describe local library approaches as go-between techniques for grafted foreign peptide sequences and small scaffold proteins, and as methods for designing high-quality libraries of small scaffold proteins.

Functionalization of small scaffold proteins by peptide grafting

The design of chimeric proteins, in which specific segments are replaced with functional sequences derived from other proteins, can give new binding abilities to scaffold proteins. A new chimeric protein can be generated by replacing the amino acid sequence in an exposed surface area with a fragment that binds a target molecule from another protein.

To generate a small binding protein by grafting, we need to visualize the tertiary structures of donor and recipient proteins in detail. In particular, visualization facilitates the identification of fragments with binding ability. The RGD motif (Arg-Gly-Asp) is a well-known fragment with binding ability. It is found in cell adhesion molecules such as fibronectin, and its interaction with a cell surface receptor called integrin has been analyzed from a structural viewpoint [10–12]. Its short sequence is attractive for generating small binding proteins by grafting. Grafting of the motif with its neighboring sequences from fibronectin into an exposed loop in lysozyme functionalized lysozyme without inactivating its enzyme function [13]. The grafting gave lysozyme low binding affinity for cell surface receptors, and X-ray and NMR structural analyses demonstrated high flexibility and exposure of the grafted motif [13].

Drakopoulou *et al.* [14] noted the resemblance of loop structures with binding ability between scorpion charybdotoxin (with affinity for potassium ion channel protein) and snake toxin α (with affinity for acetylcholine receptor), and replaced a loop sequence of charybdotoxin with one of toxin α to express a new binding function. Comparison of the X-ray crystal structures between charybdotoxin and toxin α showed the structural resemblance of the β-hairpin loop with binding function between toxins. The grafting of the toxin α loop structure into charybdotoxin caused little structural change, and gave charybdotoxin affinity for the

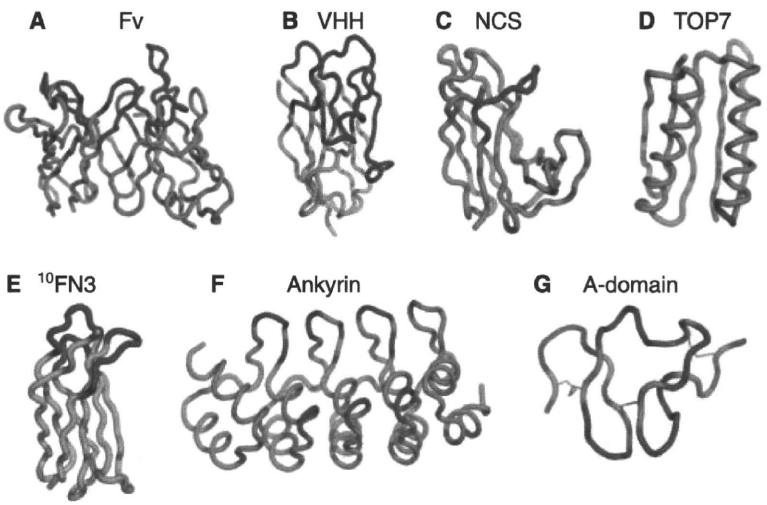

Fig. 1. Structures of small scaffold proteins as specific binders. Red loops are the appropriate locations that can have binding functions through peptide-grafting or local library approaches.

acetylcholine receptor instead of the potassium ion channel protein, albeit with lower binding affinity, as seen above with the grafting of RGD into lysozyme.

Recently, stable, small scaffold proteins with surface loop structures that can bind to another protein have been reported. Neocarzinostatin (NCS), found in *Streptomyces neocarzinostaticus*, is a candidate scaffold protein with a hydrophilic and IgG-like structure (Fig. 1C) [15,16]. Visualization of antigen–antibody complexes by X-ray crystallography shows that hypervariable complementarity-determining region (CDR) loops on a fragment of the variable region (Fv) of antibodies recognize specific antigen surfaces (red loops in Fig. 1A) [17–19]. Nicaise *et al.* [20] searched for the most suitable location in NCS for grafting the CDR loop of the single variable heavy chain of a heavy-chain camel antibody (VHH) (Fig. 1B) by comparing topologies between VHH and NCS (Fig. 2A); grafting of the CDR 3 loop of antilysozyme VHH functionalized NCS without denaturation, although the thermal stability was decreased and the affinity for lysozyme was weaker than in the original VHH.

The computer-designed TOP protein is an α/β-protein composed of 93 amino acids without disulfide linkages (Fig. 1D) [21]. This artificial protein is so thermophilic that it is not denatured at 98 °C, and it can be expressed at a high level in *Escherichia coli*. Boschek *et al.* [22] grafted the CDR 1-containing loop of the heavy chain (CDR H1) of antibody against CD4 into a loop structure of TOP that was identified by molecular dynamics simulation as a suitable location without denaturation (Fig. 2B). CDR-grafted TOP had affinity for CD4 receptor, and was not denatured even at 95 °C.

Combining grafting and local library approaches for high-affinity scaffold proteins

The grafting results demonstrate the utility of the structural information supplied by X-ray and NMR analyses for functionalizing small scaffold proteins. However, this structural information is not enough to support the complete transfer of functions.

Fv of antibodies is a well-studied small scaffold protein. Fv has a flexible and stable framework with hypervariable sequences and lengths in the six-loop CDR (Fig 1A) that bind to the antigen. The first study of grafting into the CDR replaced the CDR loops in a human antibody with those from a mouse antibody to avoid immunogenicity of the antibody framework from a different species [23–25]. The success of the series of studies shows that the stable framework structure of Fv enables the transfer of function by means of CDR replacement.

Barbas *et al.* first designed new functional antibody fragments by grafting the RGD motif in CDR loops [26,27]. Recognizing that functionalization by grafting RGD needs designs for adjusting the orientation of the RGD motif, they grafted XXXRGDXXX peptide sequences, in which the X positions were randomized, into the CDR 3 loop in the heavy chain (CDR H3) of Fv to select sufficiently functionalized Fab fragments by using phage display methods (Fig. 3A); clone Fab 9 had a low equilibrium dissociation constant (K_d) of 0.25 nM, comparable to that of vitronectin. This result implies that the library approach is important for the design of edge sequences neighboring to the grafted peptide fragment to fully functionalize scaffold proteins.

Fab 9 was also attractive as a supplier of the peptide sequence with affinity for a specific molecule. Smith *et al.* [28] reported the grafting of a CDR fragment into a loop structure of a small scaffold protein. When the CDR H3 loop of Fab 9 was grafted into a long, surface-exposed loop structure in a human tissue-type plasminogen activator with affinity for fibrin, the new plasminogen activator had comparable affinity for integrin to that of Fab 9, with no loss of fibrin-binding function.

Although peptide fragments have often been grafted into CDR H3, because its length and amino acid

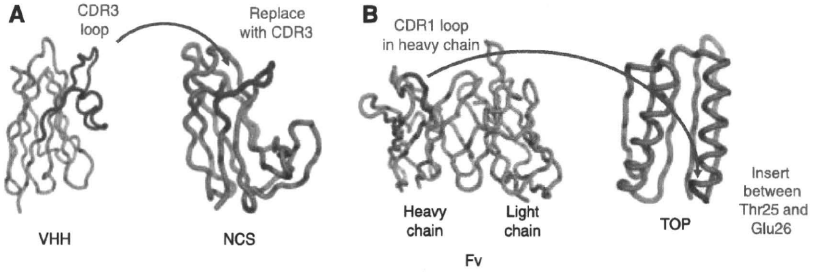

Fig. 2. Functionalization of small scaffold proteins by replacing a loop of the scaffold protein with a CDR loop of antibody fragments. (A) Replacement of the candidate location in NCS for grafting with the CDR 3 loop of VHH. (B) Insertion of the CDR 1-containing loop of the heavy chain in Fv into the candidate location in TOP.

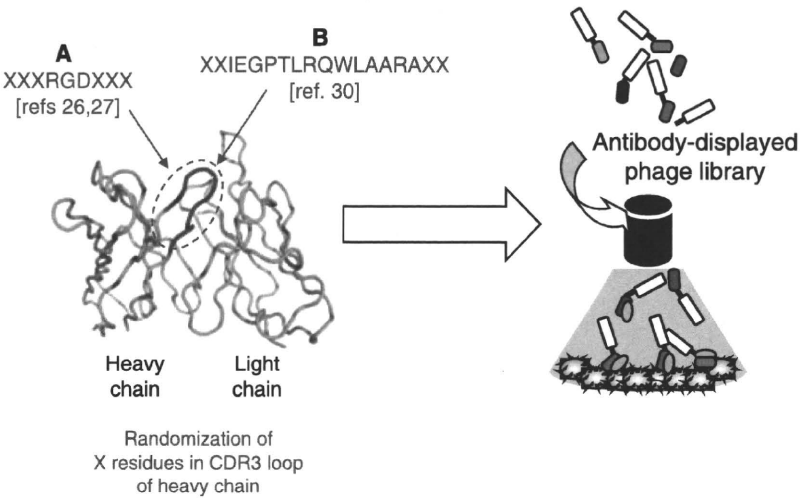

Fig. 3. Combination of grafting and local library approaches in CDR 3 loops of the heavy chain to select high-affinity Fv by using the phage display method.

sequence are highly variable, a few studies of grafting into other CDR loops have also been reported. Simon *et al.* [29] grafted the receptor-binding site sequence of somatostatin, which binds to somatostatin receptor 5, into the CDR 1 and CDR 2 loops in the light chain (CDR L1 and CDR L2) to study the potential of Fv as a scaffold protein for grafting. They investigated deviations in the amino acid sequences of the CDRs of 1330 human light chains to identify the candidate residues important in the light chain conformation. Peptide grafting into locations with no significance for light chain folding functionalized the antibody fragments, but expression of the fragment was decreased and the binding affinity was weakened. This might imply the importance of library approaches in specific local areas to overcome the problems not resolved by visualized structural information alone.

The stability of Fvs as scaffold proteins also enables the design of new functional antibody fragments from peptide sequences selected from peptide libraries. A peptide with high affinity for thrombopoietin (TPO), which was selected from a peptide library by the use of phage display method, was grafted into the CDR H3 loop in human Fabs [30]. Grafting of the TPO-binding peptide with two randomized residues at the edge terminus enabled selection of a high-affinity Fab (Fig. 3B), demonstrating the utility of the grafting of functional peptides with randomized edge sequences for optimizing the orientation of the grafted peptide on a scaffold protein. In addition, when the combination of grafting and local library approaches was applied to other CDR loops in Fabs with TPO-binding peptide grafted onto CDR H3, a clone of the double-grafted Fabs had not only higher affinity, but also bivalent function [30]: the grafted Fab had agonist activity caused by the dimerization of the TPO-binding peptide.

The combination of grafting and local library methods is suitable for generating binding proteins. In particular, bispecific small proteins, such as Fabs with dual affinity for human epidermal growth factor receptor 2 and vascular endothelial growth factor (VEGF) [31], might be achievable by grafting two different functional peptide sequences. Recently, several peptides with affinity for inorganic material surfaces have been selected from a peptide library, and the replacement of material-binding peptide with the CDR 1 loop of VHH and the local library approach in the CDR 3 loop generated the VHH fragments with high affinity for specific inorganic material surfaces [32]. The combination of grafting and local library methods might also be suitable for generating specific binders against unexplored targets.

Local artificial library in a small scaffold protein

Detailed tertiary structural information obtained by X-ray and NMR techniques not only enables grafting approaches for the functionalization of small scaffold proteins, but also opens the way to direct functionalization of scaffold proteins by the use of artificial libraries. Functionalizing a small scaffold protein by a library approach requires large-scale, high-quality libraries with correctly folded variants of scaffold proteins. If the rate of correctly folded variants in a library were low, the number of functional variants in the library would be extremely low. Native libraries of antibodies, such as immune and naive libraries, are considered to hold correctly folded variants; but for the construction of artificial libraries,

randomized locations in scaffold proteins and diversity of amino acids in libraries should be carefully considered.

In the use of artificial libraries for generating binding proteins, Fvs of antibodies are most commonly used as scaffold proteins. In the case of single-chain Fvs and Fabs, artificial libraries of CDR loops have been constructed from synthetic DNA fragments with randomized sequences and lengths. The first attempt with artificial libraries did not provide high-affinity antibody fragments [33], but increasing the library scale to $\sim 10^{11}$ enabled the selection of fragments with high affinity for various protein antigens and haptens [34]. The construction of very large libraries is effective, because it increases the number of correctly folded variants [35]. To decrease the number of misfolded, unfolded and aggregated variants in the libraries, efficient libraries mimicking the frequency of amino acids in native CDR loops have been constructed on one or more frameworks [36,37].

Recently, amino acid-restricted libraries, in which CDR loops were randomized using only the amino acids frequently found in native CDR, have been constructed to increase the density of libraries (Fig. 4A). Fabs with high affinity for human VEGF were selected from a restricted library constructed from only Tyr, Ser, Asp, and Ala, and X-ray structural analysis demonstrated the importance of Tyr residues [38]. The construction of more restricted libraries from only Tyr and Ser residues (YS binary code libraries) also enabled the selection of high-affinity antibodies [39]: one Fab had high affinity for human VEGF (K_d = 60 nM). X-ray structural analysis of the complex of another Fab and human death receptor 5 confirmed the importance of Tyr residues in the antigen–antibody interface.

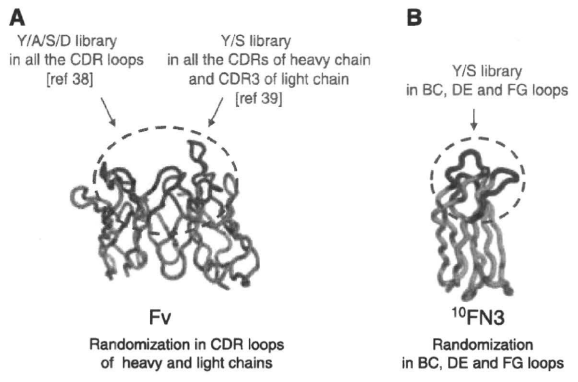

Fig. 4. Local artificial library design in (A) CDR loops of Fv and (B) BC, DE and FG loops of ^{10}FN3 to select high-affinity small scaffold proteins.

Artificial library approaches are also effective with nonantibody proteins when the tertiary structures of scaffold proteins are analyzed in detail. The 10th fibronectin type III domain (^{10}FN3) of human fibronectin (Fig. 1E), which is a component of the extracellular matrix, is a monomer with a similar β-sandwich structure to the IgG fold, and has three loops [12]. Koide *et al.* [40] reported the construction of nonantibody-binding proteins, called monobodies, by randomizing the sequences of the loops in ^{10}FN3 (Fig. 4B). Monobodies with a wide range of affinities (picomolar to micromolar K_d values) have been reported. Xu *et al.* [41] selected a monobody with a K_d of 20 pM for tumor necrosis factor-α by mRNA display from an extremely large library (10^{12} unique clones). Lipovšek *et al.* [42] selected anti-lysozyme monobodies with a low K_d value of 350 pM by yeast surface display from a small library (10^7–10^9 unique clones). A YS binary code library has also allowed selection of monobodies with affinity for maltose-binding protein and small ubiquitin-like modifier [43], indicating the effectiveness of the amino acid-restricted library approach even with nonantibody scaffold proteins. X-ray structural analysis of monobodies selected from the YS binary library again indicated the importance of Tyr residues for binding to target molecules [43]. Tyr residues might play an important role in molecular recognition independently of scaffold proteins. The generation of recombinant binding proteins by library approaches will supply new insights into protein–protein interactions, and the information might suggest novel designs for high-quality artificial libraries.

Construction of high-affinity-binding proteins by multispecific design

Tertiary structural information on antibody fragments and nonantibody small scaffold proteins from X-ray and NMR analyses enables the design of and screening for small binding proteins. The preparation of the small binding proteins with binding function further allows us to increase the binding strength by multi-binding approaches, constructing multispecific proteins from two small proteins with different epitopes in a target molecule [44,45].

Neri *et al.* [44] created a bispecific antibody fragment with two single-chain Fvs (scFvs), each of which binds to a nonoverlapping epitope in lysozyme, called chelating recombinant antibody (CRAb). The polypeptide linker via which the two scFvs were tandemly connected was designed by computer graphic modeling, using tertiary structures of the antigen–antibody complexes, with the result that the CRAb with D1.3 and

mutant HyHEL-10 scFvs had 100-fold the affinity of either of the scFvs alone. Local library approaches have also been attempted for the design of appropriate polypeptide linkers with a repeat unit of $(XGGGS)_n$, in which the residues at X were randomized and the linker length (n) was intermittently varied from 11 to 54 (Fig. 5A) [46]. Selection from the tandem-scFv-displayed phage libraries led to the enrichment of CRAbs with linker lengths comparable to those obtained with computer graphic modeling. The linker library approach has potential for the design of CRAbs when the exact relative positions of two epitopes are indefinite, and for application to nonantibody scaffold proteins.

Several recent studies have reported the simultaneous operation of generating small binding polypeptide units and incrementing the units to achieve multibinding on a target molecule. Designed ankyrin repeat protein (DARPin) is a protein constructed from the ankyrin repeat unit (Fig. 1F) [47]. The unit has 33 amino acids, without internal disulfide linkages, and it forms a β-turn followed by two antiparallel helices and a loop reaching the β-turn of the next repeat. The number of replications is changed so that small binding proteins with appropriate multibinding effects can be generated from units recognizing different epitopes. The randomization of six amino acids in the loop and helix structures without Cys, Gly or Pro enabled the selection of DARPin variants with high affinity for maltose-binding protein [48], Her2 [49,50], and mitogen-activated protein kinase (Fig. 5B) [51].

The A-domain is a small scaffold protein that can be used as a repeat unit (Fig. 1G) [52–54]. A-domains consisting of ~ 35 amino acids occur in strings of multiple domains in several cell surface receptors, and are connected via several amino acid linkers. Each A-domain in the multimer binds to different epitopes in a target, generating avidity [55]. Twelve amino acids that form disulfide linkages and coordinate calcium ions are conserved in ~ 200 human A-domains, but other residues are highly variable [56]. By repeating randomization of the variable residues, selection of A-domain variants with affinity for a target, and connection between the selected variants (Fig. 5C), Silverman *et al.* [57] selected avidity multimers called avimers with two or three A-domains with high affinity (nanomolar K_d) for interleukin-6, CD40L, and CD28.

Conclusions and outlook

Accurate structural descriptions of protein–protein complexes provide support for the replacement of binding site sequences and thus binding function between structurally similar proteins. Functionalization by grafting is not perfect, because structural information derived only from X-ray and NMR analyses is not enough to avoid the decrease in affinity, but some local library approaches can compensate. The identification of the binding site on a protein from visualized tertiary structures can lead to the construction of an efficient library with a low probability of denatured variants, and its combination with the design for library diversity opens the way to increasing the size of the amino acid sequence that can be randomized without decreasing the density of the library. Detailed tertiary structural analyses of protein–protein complexes further accurately describe epitope locations, enabling the design of and screening for bispecific high-affinity proteins recognizing different epitopes in a target molecule.

The recent explosive increase in new genomic and protein structural information has revealed various

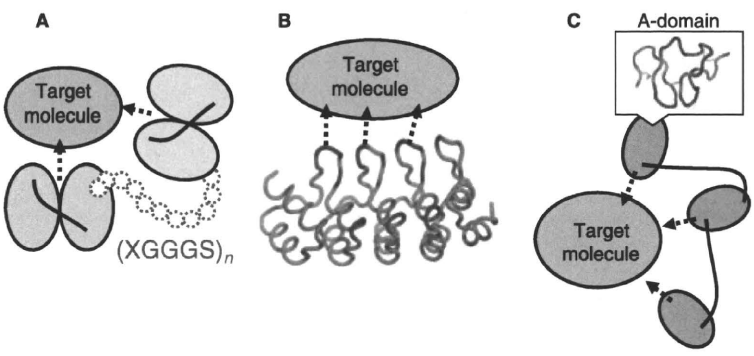

Fig. 5. Selection of multispecific binders with multiple binding sites for different epitopes. The red loops are randomized to select high-affinity binders with the binding sites for multiepitopes (black arrows). (A) Tandem scFv: two scFvs were tandemly connected via a repeat unit of $(XGGGS)_n$ in which the X residues were randomized and the linker length (n) was intermittently varied. (B) DARPin: six amino acids in the loop and helix structures are randomized. (C) A-domains: variable residues in each A-domain are repeatedly randomized.

small scaffold proteins of a size suitable for *in vitro* selection methods such as phage display [58,59]. The generation of recombinant binding proteins from small scaffold proteins will also help to explain the mechanism of protein–protein interactions. Consequently, analysis might suggest novel designs for high-quality artificial libraries.

Binding proteins can be used in research, diagnosis, and therapy. In particular, their therapeutic use could supply novel protein medicines that could be efficiently produced in bacterial hosts; many successful therapeutic antibodies with large and multidomain IgG formats are difficult and expensive to manufacture. However, the immunogenicity of small scaffold proteins and their very short serum half-life, owing to their small molecular size, must be overcome. Library approaches might serve the dual purposes of increasing both affinity and size.

References

1 Winter G, Griffiths AD, Hawkins RE & Hoogenboom HR (1994) Making antibodies by phage display technology. *Annu Rev Immunol* **12**, 433–455.

2 Watanabe H, Tsumoto K, Taguchi S, Yamashita K, Doi Y, Nishimiya Y, Kondo H, Umetsu M & Kumagai I (2007) A human antibody fragment with high affinity for biodegradable polymer film. *Bioconjug Chem* **18**, 645–651.

3 Watanabe H, Nakanishi T, Umetsu M & Kumagai I (2008) Human anti-gold antibodies: biofunctionalization of gold nanoparticles and surfaces with anti-gold antibodies. *J Biol Chem* **283**, 36031–36038.

4 Adams GP & Weiner LM (2005) Monoclonal antibody therapy of cancer. *Nat Biotechnol* **23**, 1147–1157.

5 Sharkey RM, Cardillo TM, Rossi EA, Chang CH, Karacay H, McBride WJ, Hansen HJ, Horak ID & Goldenberg DM (2005) Signal amplification in molecular imaging by pretargeting a multivalent, bispecific antibody. *Nat Med* **11**, 1250–1255.

6 Carter P & Merchant AM (1997) Engineering antibodies for imaging and therapy. *Curr Opin Biotechnol* **8**, 449–454.

7 Holt LJ, Enever C, de Wildt RM & Tomlinson IM (2000) The use of recombinant antibodies in proteomics. *Curr Opin Biotechnol* **11**, 445–449.

8 Ishii J, Fukuda N, Tanaka T, Ogino C & Kondo A (2010) Protein–protein interactions and selection: yeast-based approaches that exploit guanine nucleotide-binding protein signaling. *FEBS J* **277**, 1982–1995.

9 Tomizaki K, Usui K & Mihara H (2010) Protein–protein interactions and selection: array-based techniques for screening disease-associated biomarkers in predictive/early diagnosis. *FEBS J* **277**, 1996–2005.

10 Pierschbacher MD & Ruoslahti E (1984) Cell attachment activity of fibronectin can be duplicated by small synthetic fragments of the molecule. *Nature* **309**, 30–33.

11 Leahy DJ, Hendrickson WA, Aukhil I & Erickson HP (1992) Structure of a fibronectin type III domain from tenascin phased by MAD analysis of the selenomethionyl protein. *Science* **258**, 987–991.

12 Main AL, Harvey TS, Baron M, Boyd J & Campbell ID (1992) The three-dimensional structure of the tenth type III module of fibronectin: an insight into RGD-mediated interactions. *Cell* **71**, 671–678.

13 Yamada T, Matsushima M, Inaka K, Ohkubo T, Uyeda A, Maeda T, Titani K, Sekiguchi K & Kikuchi M (1993) Structural and functional analyses of the Arg-Gly-Asp sequence introduced into human lysozyme. *J Biol Chem* **268**, 10588–10592.

14 Drakopoulou E, Zinn-Justin S, Guenneugues M, Gilqin B, Menez A & Vita C (1996) Changing the structural context of a functional beta-hairpin. Synthesis and characterization of a chimera containing the curaremimetic loop of a snake toxin in the scorpion alpha/beta scaffold. *J Biol Chem* **271**, 11979–11987.

15 Adjadj E, Quiniou E, Mispelter J, Favaudon V & Lhoste JM (1992) Three-dimensional solution structure of apo-neocarzinostatin from Streptomyces carzinostaticus determined by NMR spectroscopy. *Eur J Biochem* **203**, 505–511.

16 Gao X (1992) Three-dimensional solution structure of apo-neocarzinostatin. *J Mol Biol* **225**, 125–135.

17 Braden BC & Poljak RJ (1995) Structural features of the reactions between antibodies and protein antigens. *FASEB J* **9**, 9–16.

18 Davies DR & Cohen GH (1996) Interactions of protein antigens with antibodies. *Proc Natl Acad Sci USA* **93**, 7–12.

19 Kondo H, Shiroishi M, Matsushima M, Tsumoto K & Kumagai I (1999) Crystal structure of anti-Hen egg white lysozyme antibody (HyHEL-10) Fv–antigen complex. Local structural changes in the protein antigen and water-mediated interactions of Fv–antigen and light chain–heavy chain interfaces. *J Biol Chem* **274**, 27623–27631.

20 Nicaise M, Valerio-Lepiniec M, Minard P & Desmadril M (2004) Affinity transfer by CDR grafting on a non-immunoglobulin scaffold. *Protein Sci* **13**, 1882–1891.

21 Kuhlman B, Dantas G, Ireton GC, Varani G, Stoddard BL & Baker D (2003) Design of a novel globular protein fold with atomic-level accuracy. *Science* **302**, 1364–1368.

22 Boschek CB, Apiyo DO, Soares TA, Engelmann HE, Pefaur NB, Straatsma TP & Baird CL (2009) Engineering an ultra-stable affinity reagent based on Top7. *Protein Eng Des Sel* **22**, 325–332.

23 Jones PT, Dear PH, Foote J, Neuberger MS & Winter G (1986) Replacing the complementarity-determining regions in a human antibody with those from a mouse. *Nature* **321**, 522–525.
24 Co MS, Deschamps M, Whitley RJ & Queen C (1991) Humanized antibodies for antiviral therapy. *Proc Natl Acad Sci USA* **88**, 2869–2873.
25 Makabe K, Nakanishi T, Tsumoto K, Tanaka Y, Kondo H, Umetsu M, Sone Y, Asano R & Kumagai I (2008) Thermodynamic consequences of mutations in vernier zone residues of a humanized anti-human epidermal growth factor receptor murine antibody, 528. *J Biol Chem* **283**, 1156–1166.
26 Barbas CF 3rd, Languino LR & Smith JW (1993) High-affinity self-reactive human antibodies by design and selection: targeting the integrin ligand binding site. *Proc Natl Acad Sci USA* **90**, 10003–10007.
27 Smith JW, Hu D, Satterthwait A, Pinz-Sweeney S & Barbas CF 3rd (1994) Building synthetic antibodies as adhesive ligands for integrins. *J Biol Chem* **269**, 32788–32795.
28 Smith JW, Tachias K & Madison EL (1995) Protein loop grafting to construct a variant of tissue-type plasminogen activator that binds platelet integrin alpha IIb beta 3. *J Biol Chem* **270**, 30486–30490.
29 Simon PJ, Brogle KC, Wang B, Kyle DJ & Soltis DA (2005) Display of somatostatin-related peptides in the complementarity determining regions of an antibody light chain. *Arch Biochem Biophys* **440**, 148–157.
30 Frederickson S, Renshaw MW, Lin B, Smith LM, Calveley P, Springhorn JP, Johnson K, Wang Y, Su X, Shen Y *et al.* (2006) A rationally designed agonist antibody fragment that functionally mimics thrombopoietin. *Proc Natl Acad Sci USA* **103**, 14307–14312.
31 Bostrom J, Yu SF, Kan D, Appleton BA, Lee CV, Billeci K, Man W, Peale F, Ross S, Wiesmann C *et al.* (2009) Variants of the antibody herceptin that interact with HER2 and VEGF at the antigen binding site. *Science* **323**, 1610–1614.
32 Hattori T, Umetsu M, Nakanishi T, Togashi T, Yokoo N, Abe H, Ohara S, Adschiri T & Kumagai I (2010) High-affinity anti-inorganic-material antibody generation by integrating graft and evolution technologies: the potential of antibodies as biointerface molecules. *J Biol Chem* **285**, 7784–7793.
33 Nissim A, Hoogenboom HR, Tomlinson IM, Flynn G, Midgley C, Lane D & Winter G (1994) Antibody fragments from a 'single pot' phage display library as immunochemical reagents. *EMBO J* **13**, 692–698.
34 Griffiths AD, Williams SC, Hartley O, Tomlinson IM, Waterhouse P, Crosby WL, Kontermann RE, Jones PT, Low NM, Allison TJ *et al.* (1994) Isolation of high affinity human antibodies directly from large synthetic repertoires. *EMBO J* **13**, 3245–3260.
35 Christ D, Famm K & Winter G (2006) Tapping diversity lost in transformations – in vitro amplification of ligation reactions. *Nucleic Acids Res* **34**, e108, doi:10.1093/nar/gkl605.
36 Lee CV, Liang WC, Dennis MS, Eigenbrot C, Sidhu SS & Fuh G (2004) High-affinity human antibodies from phage-displayed synthetic Fab libraries with a single framework scaffold. *J Mol Biol* **340**, 1073–1093.
37 Knappik A, Ge L, Honegger A, Pack P, Fischer M, Wellnhofer G, Hoess A, Wolle J, Plückthun A & Virnekas B (2000) Fully synthetic human combinatorial antibody libraries (HuCAL) based on modular consensus frameworks and CDRs randomized with trinucleotides. *J Mol Biol* **296**, 57–86.
38 Fellouse FA, Wiesmann C & Sidhu SS (2004) Synthetic antibodies from a four-amino-acid code: a dominant role for tyrosine in antigen recognition. *Proc Natl Acad Sci USA* **101**, 12467–12472.
39 Fellouse FA, Li B, Compaan DM, Peden AA, Hymowitz SG & Sidhu SS (2005) Molecular recognition by a binary code. *J Mol Biol* **348**, 1153–1162.
40 Koide A, Bailey CW, Huang X & Koide S (1998) The fibronectin type III domain as a scaffold for novel binding proteins. *J Mol Biol* **284**, 1141–1151.
41 Xu L, Aha P, Gu K, Kuimelis RG, Kurz M, Lam T, Lim AC, Liu H, Lohse PA, Sun L *et al.* (2002) Directed evolution of high-affinity antibody mimics using mRNA display. *Chem Biol* **9**, 933–942.
42 Lipovšek D, Lippow SM, Hackel BJ, Gregson MW, Cheng P, Kapila A & Wittrup KD (2007) Evolution of an interloop disulfide bond in high-affinity antibody mimics based on fibronectin type III domain and selected by yeast surface display: molecular convergence with single-domain camelid and shark antibodies. *J Mol Biol* **368**, 1024–1041.
43 Koide A, Gilbreth RN, Esaki K, Tereshko V & Koide S (2007) High-affinity single-domain binding proteins with a binary-code interface. *Proc Natl Acad Sci USA* **104**, 6632–6637.
44 Neri D, Momo M, Prospero T & Winter G (1995) High-affinity antigen binding by chelating recombinant antibodies (CRAbs). *J Mol Biol* **246**, 367–373.
45 Zhou HX (2003) Quantitative account of the enhanced affinity of two linked scFvs specific for different epitopes on the same antigen. *J Mol Biol* **329**, 1–8.
46 Wright MJ & Deonarain MP (2007) Phage display of chelating recombinant antibody libraries. *Mol Immunol* **44**, 2860–2869.
47 Binz HK, Stumpp MT, Forrer P, Amstutz P & Plückthun A (2003) Designing repeat proteins: well-expressed, soluble and stable proteins from combinatorial libraries of consensus ankyrin repeat proteins. *J Mol Biol* **332**, 489–503.

48 Binz HK, Amstutz P, Kohl A, Stumpp MT, Briand C, Forrer P, Grutter MG & Plückthun A (2004) High-affinity binders selected from designed ankyrin repeat protein libraries. *Nat Biotechnol* **22**, 575–582.
49 Zahnd C, Pecorari F, Straumann N, Wyler E & Plückthun A (2006) Selection and characterization of Her2 binding-designed ankyrin repeat proteins. *J Biol Chem* **281**, 35167–35175.
50 Zahnd C, Wyler E, Schwenk JM, Steiner D, Lawrence MC, McKern NM, Pecorari F, Ward CW, Joos TO & Plückthun A (2007) A designed ankyrin repeat protein evolved to picomolar affinity to Her2. *J Mol Biol* **369**, 1015–1028.
51 Amstutz P, Koch H, Binz HK, Deuber SA & Plückthun A (2006) Rapid selection of specific MAP kinase-binders from designed ankyrin repeat protein libraries. *Protein Eng Des Sel* **19**, 219–229.
52 Krieger M & Herz J (1994) Structures and functions of multiligand lipoprotein receptors: macrophage scavenger receptors and LDL receptor-related protein (LRP). *Annu Rev Biochem* **63**, 601–637.
53 Gliemann J (1998) Receptors of the low density lipoprotein (LDL) receptor family in man. Multiple functions of the large family members via interaction with complex ligands. *Biol Chem* **379**, 951–964.
54 North CL & Blacklow SC (1999) Structural independence of ligand-binding modules five and six of the LDL receptor. *Biochemistry* **38**, 3926–3935.
55 Rettenberger PM, Oka K, Ellgaard L, Petersen HH, Christensen A, Martensen PM, Monard D, Etzerodt M, Chan L & Andreasen PA (1999) Ligand binding properties of the very low density lipoprotein receptor. Absence of the third complement-type repeat encoded by exon 4 is associated with reduced binding of Mr 40,000 receptor-associated protein. *J Biol Chem* **274**, 8973–8980.
56 Koduri V & Blacklow SC (2001) Folding determinants of LDL receptor type A modules. *Biochemistry (Mosc)* **40**, 12801–12807.
57 Silverman J, Liu Q, Bakker A, To W, Duguay A, Alba BM, Smith R, Rivas A, Li P, Le H *et al.* (2005) Multivalent avimer proteins evolved by exon shuffling of a family of human receptor domains. *Nat Biotechnol* **23**, 1556–1561.
58 Binz HK, Amstutz P & Plückthun A (2005) Engineering novel binding proteins from nonimmunoglobulin domains. *Nat Biotechnol* **23**, 1257–1268.
59 Hosse RJ, Rothe A & Power BE (2006) A new generation of protein display scaffolds for molecular recognition. *Protein Sci* **15**, 14–27.

THE JOURNAL OF BIOLOGICAL CHEMISTRY VOL. 285, NO. 27, pp. 20844–20849, July 2, 2010

Highly Enhanced Cytotoxicity of a Dimeric Bispecific Diabody, the hEx3 Tetrabody*

Received for publication, March 5, 2010, and in revised form, April 21, 2010 Published, JBC Papers in Press, May 5, 2010, DOI 10.1074/jbc.M110.120444

Ryutaro Asano[‡], Keiko Ikoma[‡], Yukiko Sone[‡], Hiroko Kawaguchi[‡], Shintaro Taki[‡], Hiroki Hayashi[§], Takeshi Nakanishi[‡], Mitsuo Umetsu[‡], Yu Katayose[§], Michiaki Unno[§], Toshio Kudo[¶], and Izumi Kumagai[‡1]

From the [‡]Department of Biomolecular Engineering, Graduate School of Engineering, Tohoku University, Sendai 980-8579, Japan, the [§]Division of Gastroenterological Surgery, Department of Surgery, Graduate School of Medicine, Tohoku University, Sendai 980-8574, Japan, and the [¶]Cell Resource Center for Biomedical Research, Institute of Development, Aging, and Cancer, Tohoku University, Sendai 980-8575, Japan

We previously reported the utility for cancer immunotherapy of a humanized bispecific diabody (hEx3) that targets epidermal growth factor receptor and CD3. Here, we used dynamic and static light scattering measurements to show that the multimer fraction observed in hEx3 in solution is a monodisperse tetramer. The multimerization into tetramers increased the inhibition of cancer cell growth by the hEx3 diabody. Furthermore, 1:2 stoichiometric binding for both antigens was observed in a thermodynamic analysis, indicating that the tetramer has bivalent binding activity for each target, and the structure may be in a circular configuration, as is the case for the single-chain Fv tetrabody. In addition to enhanced cytotoxicity, the functional affinity and stability of the hEx3 tetrabody were superior to those of the hEx3 diabody. The increase in molecular weight is also expected to improve the pharmacokinetics of the bispecific diabody, making the hEx3 tetrabody attractive as a therapeutic antibody fragment for cancer immunotherapy.

Bispecific antibodies (BsAbs)[2] are recombinant antibodies that can bind to two different antigenic epitopes. Bispecificity can be used in cancer immunotherapy to cross-link tumor cells to immune cells such as cytotoxic T cells, natural killer cells, and macrophages. This cross-linking accelerates the destruction of the tumor cells by the immune cells, which may translate into improved antitumor therapy and lower production costs by decreasing the doses needed (1, 2). However, the use of BsAbs in clinical studies has been hampered by difficulties in producing them on a large scale. Conventional chemical conjugation has been used, but the quality of the antibody produced is inconsistent (3). The production of BsAbs by somatic fusion of two hybridomas to form a quadroma yields BsAbs of more consistent quality but results in the formation of various chain-shuffled antibodies; for instance, 10 different antibodies can be generated after random association of two heavy and two light chains (4, 5).

Advances in recombinant technology have made it feasible to generate small recombinant BsAbs constructed from two different variable antibody fragments. Bispecific diabodies are the smallest available BsAbs, and the distance between the two antigen-binding sites is sufficient to link two cells (6, 7). The effectiveness of bispecific diabodies in cancer therapy has been shown extensively in *in vitro* and *in vivo* models (8–10). We also have constructed functional bispecific diabodies (11, 12). In particular, the humanized bispecific diabody hEx3 has marked antitumor activity and can retarget lymphokine-activated killer cells with the T cell phenotype (T-LAK cells) against epidermal growth factor receptor (EGFR)-positive cell lines (13, 14). The compact structure of bispecific diabodies contributes to low immunogenicity, high tumor penetration, and the potential for large scale preparation through bacterial expression systems; however, the downsizing results in rapid clearance from blood. In addition, the structure contains only one binding domain for each target, which results in low functional affinity (15, 16).

Multimerization of small recombinant antibodies is one available strategy for improving their pharmacokinetic and binding affinity. In single-chain Fvs (scFvs), the length and composition of the polypeptide linker between the variable heavy (VH) and light (VL) domains strongly influence the formation of the multimeric structure. A linker of 15 amino acid residues leads to the formation of an scFv, but reducing the linker length to 8–12 residues causes the scFvs to assemble into dimers, so that diabodies are formed. A further reduction to less than five residues leads to the formation of scFv trimers or tetramers (known as triabodies or tetrabodies) (17–21). These scFv multimers are larger and have higher valency than the monomeric form; consequently, their clearance from circulation and accumulation on tumors are improved (22, 23).

Bispecific diabodies are generally produced from heterodimerization of two different hetero-scFvs (*e.g.* VH_A-VL_B and VH_B-VL_A) with a glycine-rich linker (GGGGS; 8, 24). The hetero scFvs can also form higher multimeric structures (25), and the multimeric bispecific diabodies formed are expected to

* This work was supported by grants-in-aid for scientific research from the Ministry of Education, Science, Sports, and Culture of Japan (to R. A. and I. K.) and by grants from the New Energy and Industrial Technology Development Organization (NEDO) of Japan. This work was also supported by the Program for Promotion of Fundamental Studies in Health Sciences of the National Institute of Biomedical Innovation.

[1] To whom correspondence should be addressed: Aoba 6-6-11-606, Aramaki, Aoba-ku, Sendai 980-8579, Japan. Fax: 81-22-795-6164; E-mail: kmiz@kuma.che.tohoku.ac.jp.

[2] The abbreviations used are: BsAbs, bispecific antibodies; DLS, dynamic light scattering; EGFR, epidermal growth factor receptor; ITC, isothermal titration calorimetry; MTS, 3-(4,5-dimethylthiazole-2-yl)-5-(3-carboxymethoxyphenyl)-2-(4-sulfophenyl)-2*H*-tetrazolium inner salt; scDb, single-chain diabody; scFv, single-chain Fv; sEGFR, soluble EGFR; SLS, static light scattering; T-LAK, lymphokine-activated killer cells with the T-cell phenotype; tanDb, tandem single-chain diabody.

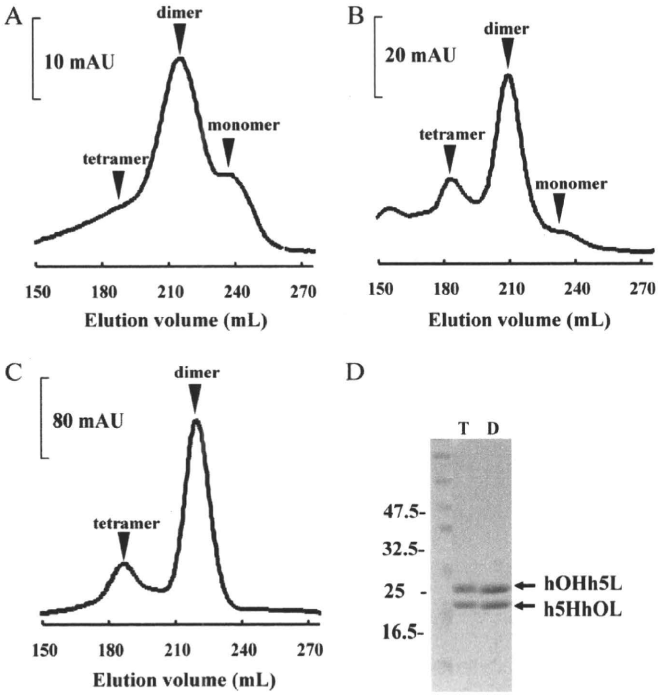

FIGURE 1. **Gel filtration of hEx3 prepared with three different methods.** The elution volume is noted on the *x* axis. *A*, hEx3 from a refolding system (13); *B*, hEx3 from a mammalian expression system (14); and *C*, hEx3 from an Fc fusion format (27). *D*, SDS-PAGE analysis of the eluted fractions under reducing conditions. The tetramer (*T*) and dimer (*D*) fractions of hEx3 from the Fc fusion format are shown. *mAU*, milli-absorbance unit.

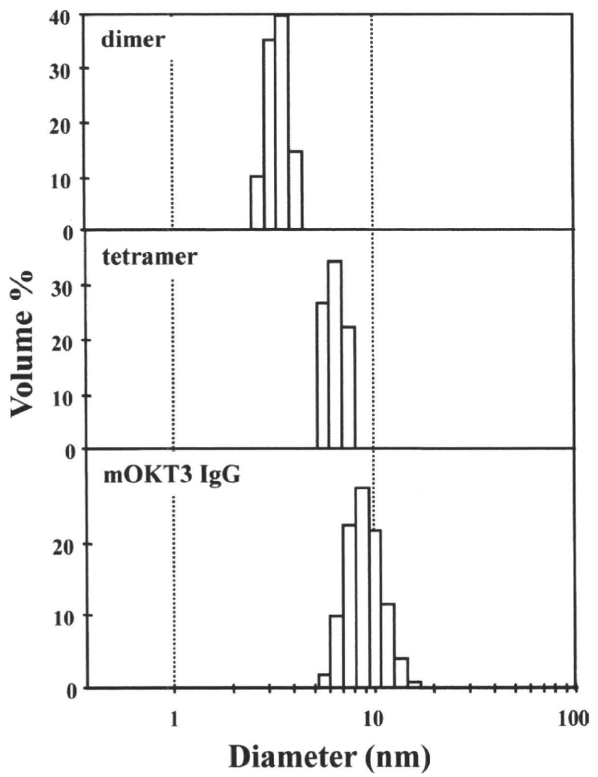

FIGURE 2. **Distributions of hydrodynamic diameters determined with the DLS histogram method.**

have multivalent bispecificity and appropriate molecular weight. Here, we examined the multimerization of hEx3 by preparing monodisperse tetramers (hEx3 tetrabodies). These

TABLE 1
Diameter and molecular mass of antibodies evaluated by DLS and SLS

	Calculated MM[a]	Diameter from DLS (distribution)	MM from SLS
	kDa	*nm*	*kDa*
dimer	53	3.43 (2.7–4.19)	n.d.[b]
tetramer	106	6.57 (4.85–10.1)	111
mOKT3 IgG	150	9.07 (5.61–15.7)	156

[a] MM, molecular mass.
[b] n.d., not determined.

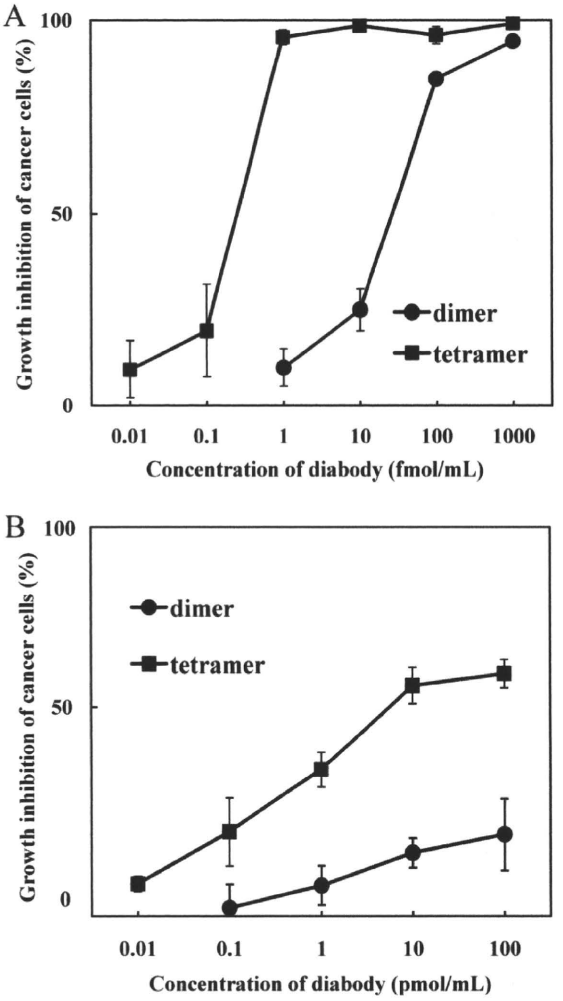

FIGURE 3. **Growth inhibition of EGFR-positive TFK-1 cells by the dimeric and tetrameric fractions of hEx3.** *A*, hEx3s and T-LAK cells were added to TFK-1 cells at a ratio of 5:1. *B*, hEx3s and peripheral blood mononuclear cells were added to TFK-1 cells at a ratio of 10:1. Data are presented as the mean value ± S.D. and are representative of at least three independent experiments with similar results.

bispecific tetrabodies had much higher affinity for each antigen than normal diabodies due to an avidity effect, which led to strong inhibition of cancer cell growth. To our knowledge, this is the first detailed quantitative characterization of functional bispecific tetrabodies.

EXPERIMENTAL PROCEDURES

Preparation of Recombinant BsAbs—For the expression and preparation of hEx3, we used three different methods in accordance with previous reports: a preparation using a bacterial expres-

TABLE 2

K_A value and stoichiometry (*n*) for sEGFR and CD3εγ evaluated by ITC

m528 IgG and Fab were used for sEGFR, and mOKT3 IgG and Fab were used for CD3εγ.

	sEGFR		CD3εγ	
	K_A ($\times 10^7$ M^{-1})	*n*	K_A ($\times 10^6$ M^{-1})	*n*
Fab	14.7	1.1	7.7	0.9
IgG	21.9	2.0	10.7	1.7
dimer	2.0	1.0	5.0	1.0
tetramer	15.7	1.8	10.4	2.1

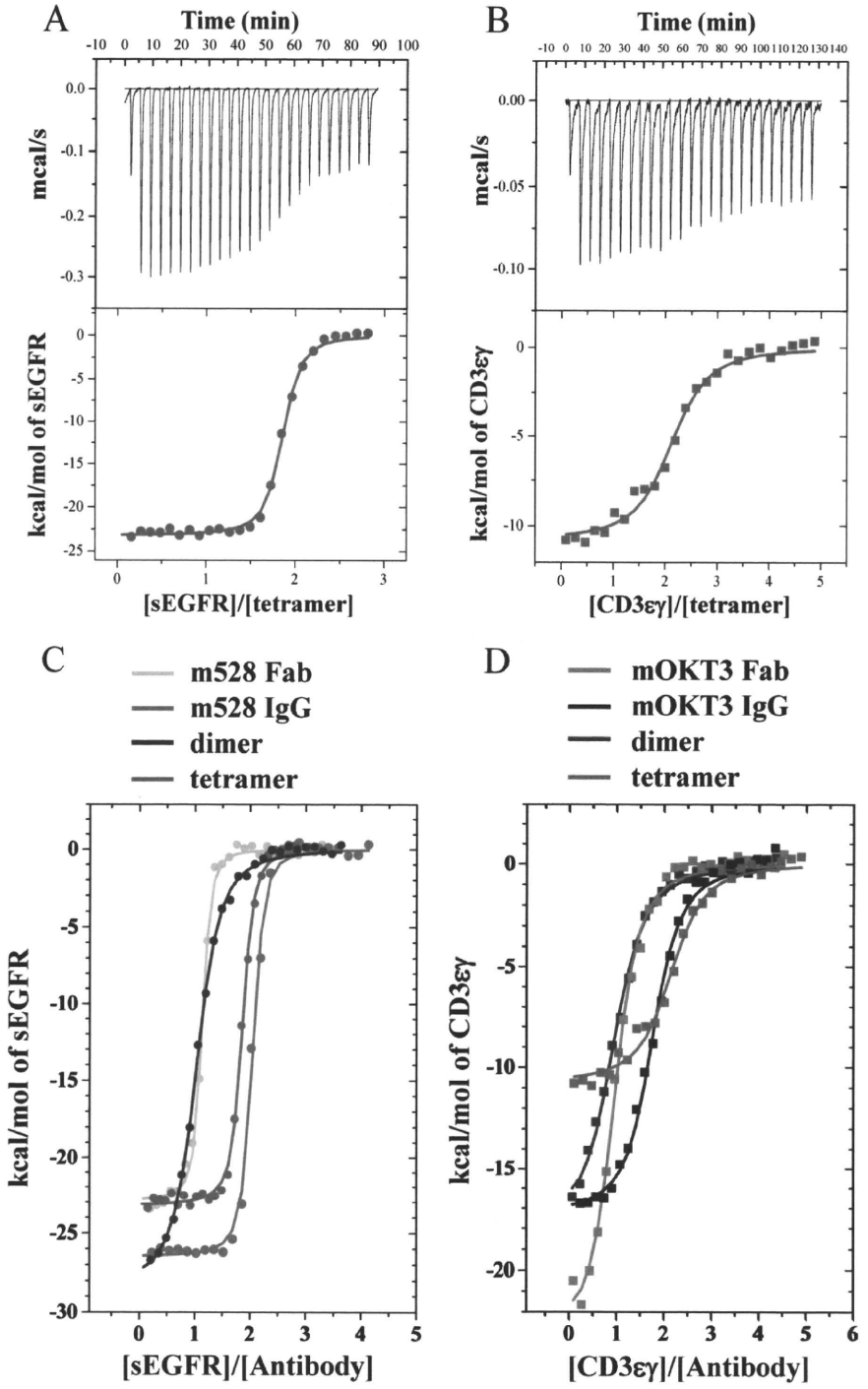

FIGURE 4. **Isothermal titration calorimetry of the interactions of antibodies with sEGFR and CD3.** Representative graphs of calorimetric titration of hEx3 tetramers at pH 7.2 and 25 °C for sEGFR (*A*) and CD3 (*B*) are shown. *C* and *D*, overlaid integration plots calculated from the raw data for Fab, IgG, hEx3 dimers, and hEx3 tetramers. The *solid lines* correspond to the best fit curves obtained by least-squares deconvolution.

sion and *in vitro* refolding system (13), a preparation using a mammalian expression system (14), and a preparation using Fc fusion format and restriction protease digestion (26, 27). Size-exclusion chromatography with a HiLoad Superdex 200-pg column (26/60; GE Healthcare) was used to fractionate each prepared hEx3 solution. The column was equilibrated with phosphate-buffered saline (PBS), and then 5 ml of purified recombinant antibodies was applied to the column at a flow rate of 2.5 ml/min.

Dynamic Light Scattering and Static Light Scattering Measurements—Dynamic light scattering (DLS) and static light scattering (SLS) measurements were carried out at 20 °C on a Zetasizer Nano ZS instrument (Malvern Instruments Ltd., Worcestershire, UK) using a He-Ne laser (λ = 633 nm). All of the antibody solutions were filtered through a polytetrafluoroethylene filter. For DLS, the antibody solutions at 15 μM were measured using a noninvasive back-scatter optical system, and the correlation curve was fitted using the default exponential g2(τ) fit function to estimate the hydrodynamic diameters of the antibodies. For analyzing molecular weight, SLS of the antibody solutions at 0.3–1.0 mg/ml was measured, and a Debye plot was made using the scattering intensity.

In Vitro Growth Inhibition Assay—T-LAK cells were induced as reported previously (28). In brief, peripheral blood mononuclear cells were cultured for 48 h at a density of 1×10^6 cells/ml in a medium supplemented with 100 international units/ml of recombinant human interleukin-2 (kindly supplied by Shionogi Pharmaceutical Co., Osaka, Japan) in a culture flask (A/S Nunc, Roskilde, Denmark) that was precoated with anti-CD3 monoclonal antibody (10 μg/ml).

In vitro growth inhibition of TFK-1 (human bile duct carcinoma) cells was assayed with a 3-(4,5-dimethylthiazole-2-yl)-5-(3-carboxymethoxyphenyl)-2-(4-sulfophenyl)-2*H*-tetrazolium inner salt (MTS) assay kit (CellTiter 96 AQueous nonradioactive cell proliferation assay; Promega, Madison, WI) as reported previously (28).

Isothermal Titration Calorimetry (ITC)—Thermodynamic analyses for the interactions of recombinant

antibodies for soluble EGFR (sEGFR) and CD3 were performed by microtitration calorimetry using a VP-ITC from MicroCal Inc. (Northampton, MA) (29). The method for expression and purification of sEGFR has been described previously (30). The expression vector for CD3 was kindly provided by Dr. Katsumi Maenaka (Kyushu University), and a preparation of CD3 was performed according to the previous report (31). Each sample (1.5 μM in PBS, pH 7.2, containing 0.005% Tween 20) was placed in a calorimeter cell and titrated with 30 μM sEGFR in the same buffer; for CD3, 1.25 μM hEx3 was titrated with 50 μM CD3. The ligand solution was injected 25 times in 10-μl portions over a period of 15 s. Data acquisition and subsequent nonlinear regression analysis were done in terms of a simple binding model, using the MicroCal ORIGIN 5.0 software package.

Surface Plasmon Resonance—The interactions between sEGFR and bispecific antibodies were analyzed by surface plasmon resonance spectroscopy with BIACORE 2000 (GE Healthcare). sEGFR was immobilized onto the cells in a CM5 sensor chip up to 2716 resonance units. Various concentrations of bispecific antibodies in 0.005% PBS with Tween 20 (PBS-T) were flowed over the sEGFR. The data were normalized by subtracting the response of a blank cell only with blocking. BIAevaluation software (GE Healthcare) was used to analyze the data. Kinetic parameters were calculated by a global fitting analysis with the assumptions of the 1:1 Langmuir binding model.

Stability Tests—To examine *in vitro* stability, hEx3s were preincubated at 37 °C for 1 h in human plasma. Growth inhibition relative to untreated hEx3s was then evaluated with the MTS assay.

Gel filtration analysis with a HiLoad Superdex 200-pg column (10/300) was used to evaluate the long term stability of the hEx3 tetramer in storage. After storage for 1 month at 4 °C, 250 μl of fractionated hEx3 tetramers was applied to a column equilibrated with PBS at a flow rate of 0.5 ml/min.

RESULTS

Structural Analysis of Prepared hEx3—We prepared the small recombinant bispecific antibody hEx3 using three different methods: refolding from insoluble aggregates expressed in *Escherichia coli*, secretory expression by Chinese hamster ovary cells, and Fc fusion expression by Chinese hamster ovary cells. Size-exclusion chromatography of each hEx3 preparation showed the predominant formation of dimers, but multimeric forms were also observed. The proportion of multimers varied with the method of preparation; refolded hEx3 produced only a small amount of multimers (Fig. 1*A*), whereas the secretory preparation using Chinese hamster ovary cells promoted the formation of multimeric forms, which corresponded to the fraction position of tetramers (Fig. 1*B*). Thus, hEx3 predominantly formed dimers but has the potential to form tetramers. hEx3 prepared from the Fc fusion format via restriction protease digestion also formed tetramers (Fig. 1*C*), and this method enabled the preparation of sufficient amounts of dimers and tetramers for further evaluation. The final yields of dimers and tetramers are 5 mg and 1 mg/liter culture, respectively. An SDS-PAGE analysis of the fractionated hEx3 showed that both the

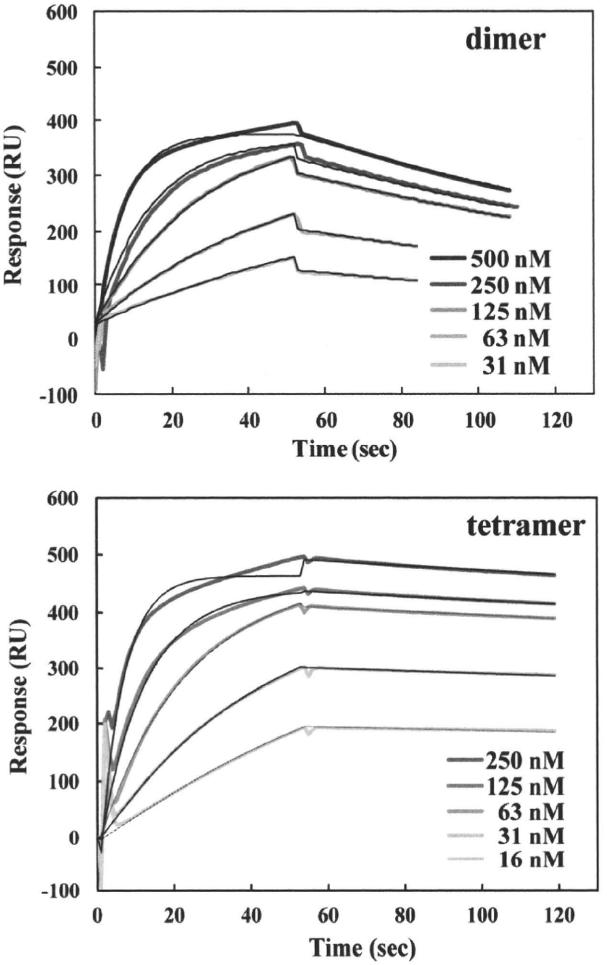

FIGURE 5. **Surface plasmon resonance sensorgrams for hEx3 dimers and tetramers.** The results from the indicated analyte concentrations are shown as *colored lines*, and global fitting kinetic analyses are shown as *black lines*. *RU*, resonance units.

anti-EGFR VH–linker–anti-CD3 VL (h5HhOL) and anti-CD3 VH–linker–anti-EGFR VL (hOHh5L) hetero-scFv fragments formed equal proportions of dimers and tetramers with all the expression methods (SDS-PAGE for hEx3 from the Fc fusion is shown in Fig. 1*D* as a representative example).

To confirm the formation of tetramers, we employed DLS and SLS spectroscopy to quantify the size and molecular weights of the dimers and tetramers fractionated from hEx3 prepared with the Fc fusion format. An IgG-type mouse anti-CD3 antibody, OKT3, was used as a control for comparison. Both the dimer and tetramer had narrow distributions, centered at 3.4 and 6.6 nm, respectively; the size of tetramer was about twice that of dimer and two-thirds that of IgG (Fig. 2 and Table 1). SLS measurement supported the molecular weight estimated from size-exclusion chromatography. Therefore, the multimer at the 190-ml fraction formed a monodisperse tetramer with equal amounts of h5HhOL and hOHh5L scFvs.

Growth Inhibition Effect of Each Fraction in hEx3 Solution—To analyze the influence of the tetramerization on the inhibition of human carcinoma cell growth, we analyzed prepared dimeric and tetrameric hEx3s with MTS. In the presence of T-LAK cells, both hEx3 forms strongly inhibited the growth of TFK-1 cells, but the tetramer was effective at a much lower

concentration, 10 fmol/ml (Fig. 3*A*). When peripheral blood mononuclear cells were applied as effector cells, although high concentrations of hEx3s were required, the tetramer also inhibited more effectively than the dimer (Fig. 3*B*). Thus, the multimerization into tetramers increased the function of hEx3.

Thermodynamic Analysis of Each Fraction of hEx3—To investigate the binding stoichiometry of each fraction in hEx3 for EGFR and CD3, we performed thermodynamic analyses by ITC. IgG and Fab were used as control molecules with bivalent and monovalent binding, respectively. The binding constants and stoichiometry are summarized in Table 2. Dimeric hEx3 showed 1:1 stoichiometric binding for EGFR (Fig. 4*C*) and CD3 (Fig. 4*D*), similar to Fab, indicating that the anti-EGFR Fv and anti-CD3 Fv portions in the dimeric hEx3 had formed correctly; that is, the prepared dimers were monomorphous diabodies without inactive homodimers. This result is consistent with our previous results supporting the formation of monomorphous hEx3 diabodies (14). In the case of tetramers, the integration plots for EGFR and CD3 showed the same binding stoichiometry as IgG but not Fab, that is, a 1:2 stoichiometric binding for both antigens (Fig. 4, *C* and *D*). The tetramer therefore formed monomorphous hEx3 tetrabodies with bivalency for two individual targets.

Comparison of Binding Kinetics with Surface Plasmon Resonance—To confirm the effect of the multivalency of tetrameric hEx3, we evaluated the binding kinetics for immobilized sEGFR by surface plasmon resonance. The binding kinetics for CD3 were not determined, because the CD3 receptors were inactivated when immobilized on a sensor chip. The sensorgram for tetrameric hEx3 against EGFR showed an association curve similar to that of the dimer, but the dissociation of the tetramer was slower than that of the dimer (Fig. 5). A global fitting to a 1:1 interactional model with a mass transport term indicated that the tetramers had an association rate similar to that of the dimers, but the dissociation rate was one-seventh of the dimer rate (Table 3); consequently, the affinity constant of the tetramer was 17-fold that of the dimer. The multimerization into a tetramer influenced the dissociation process of diabodies, resulting in increased affinity for the antigen.

Stability Test under Physiological Conditions—Physiologic stability is a critical factor for potential therapeutic recombinant proteins. Therefore, we examined the cytotoxicity of dimeric and tetrameric hEx3 after preincubation at 37 °C in human plasma. The activity of the dimers was slightly reduced; however, the intense cytotoxicity of the tetramer was retained (Fig. 6*A*). The stability of assembled structure was also evaluated by size-exclusion chromatography of the tetramer after storage for a month (Fig. 6*B*). Although a few tetramers were converted into dimers, we confirmed that the tetrameric structure was sufficiently stable for use after 1 month in storage.

TABLE 3
Binding kinetics for sEGFR evaluated with surface plasmon resonance

	k_{on}	k_{off}	K_A
	$\times 10^5\ M^{-1}\ s^{-1}$	$\times 10^{-4}\ s^{-1}$	$\times 10^7\ M^{-1}$
dimer	2.6	55.2	4.8
tetramer	6.7	8.1	81.9

DISCUSSION

Bispecific diabodies show several advantages over BsAbs produced from hybrid hybridomas or chemical conjugation; however, bispecific diabodies are also cleared rapidly, and their decrease in valence generally causes low functional affinity (15, 16). Shortening the middle linker in scFv leads to self-multimerization, and the multimerization can improve the pharmacokinetics and increase functional affinity due to an avidity effect (17–20). Multimerization of bispecific diabodies has been observed previously (25), but the effectiveness of bispecific diabodies has not been studied to date.

In the present study, we found that hEx3 formed multimers. We purified these multimers, and kinetic and thermodynamic analyses of each hEx3 fraction quantitatively demonstrated that the tetramer had two functional binding sites for each antigen (Fig. 4 and Table 2). This increase in binding sites provided strong growth inhibition activity. The multimerization was effective even for bispecific diabodies.

Engineering of linkers in single-chain diabodies (scDbs), in which two hetero-scFvs are tandemly conjugated, can provide tetravalent bispecific dimers called tandem scDbs (tanDbs). The tanDbs exhibit not only higher functional affinity

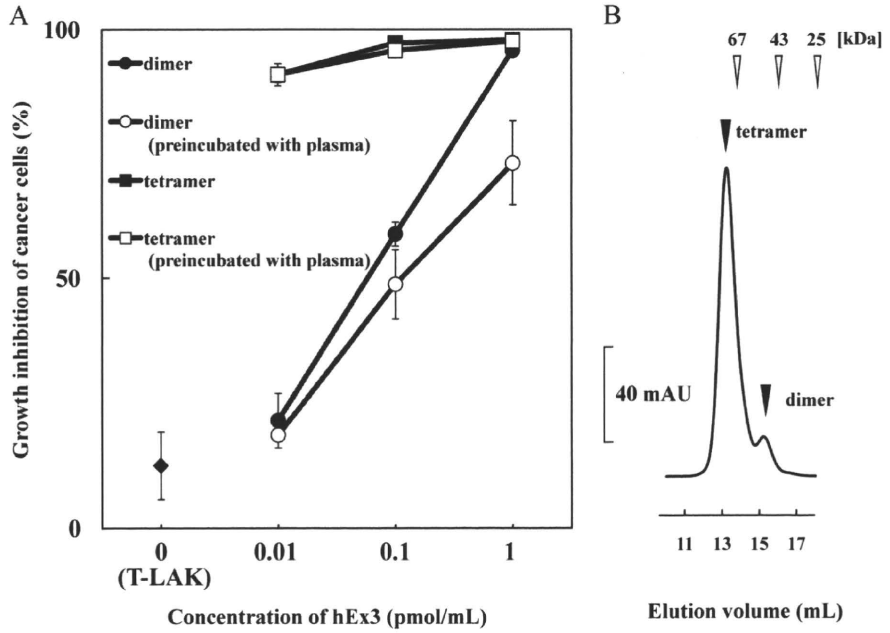

FIGURE 6. *A*, Stability test of hEx3 dimers and tetramers under physiologic conditions by assay of growth inhibition of EGFR-positive TFK-1 cells. Each bispecific antibody and T-LAK cells (effectors) was added to TFK-1 cells (targets) at a ratio of 5:1. Data are presented as the mean value ± S.D. and are representative of at least three independent experiments with similar results. *B*, gel filtration of hEx3 tetramer for confirmation of stability in storage. The elution volume is noted on the *x* axis, and the kDa values are shown above the figure. Fractionated hEx3 tetramers were applied to the column after storage for 1 month at 4 °C.

and stability under physiological conditions *in vitro* than scDbs but also longer blood retention and higher therapeutic effects *in vivo* (15, 32, 33). In this study, we prepared highly functional bispecific tetrabodies from hetero-scFv fragments with molecular sizes approximately half those of scDbs. Although the bispecific tetrabodies formed as a by-product of bispecific diabodies, the formation from smaller fragments might be an advantage in protein expression. In contrast to the structure of tanDbs, in which all four variable domains of one chain interact with the variable domains of the second chain (33, 34), the structure of the hEx3 tetramer is probably a circular structure, similar to that of the scFv tetramer (known as a tetrabody; Refs. 18, 35). We previously reported a strong interdomain interaction between the cognate VH and VL domains of hEx3 (14); this strong interaction probably contributes to the formation of a stable circular structure for the hEx3 tetrabody with four active binding sites. To date, several different small BsAb formats have been proposed to increase efficacy and availability, including not only scDb and tanDb but also tandem scFv (36) and minibodies (37). Bispecific tetrabodies like the hEx3 tetramer also should be considered small BsAb formats for the development of effective cancer therapeutic antibodies. Although *in vivo* experiments with the hEx3 tetramer are now under way, we did confirm their stability in physiologic conditions and in long term storage (Fig. 6).

In conclusion, we showed that the multimeric molecules in hEx3 solution were homogenous tetramers with high cytotoxicity. The multimerization of small antibody fragments can lead to improved pharmacokinetics and binding affinity, resulting in an enhancement of the therapeutic effect. To increase the population of hEx3 tetramers for therapeutic application, we are working to modify the middle linker in hetero-scFvs, to change the orientation of VH and VL, and to create mutations to minimize the steric interference in the tetrameric form, similar to how the scFv multimer has been modified (35, 38, 39).

REFERENCES

1. Cao, Y., and Lam, L. (2003) *Adv. Drug Deliv. Rev.* **55,** 171–197
2. Kufer, P., Lutterbüse, R., and Baeuerle, P. A. (2004) *Trends Biotechnol.* **22,** 238–244
3. Raso, V., and Griffin, T. (1981) *Cancer Res.* **41,** 2073–2078
4. Suresh, M. R., Cuello, A. C., and Milstein, C. (1986) *Methods Enzymol.* **121,** 210–228
5. Kriangkum, J., Xu, B., Nagata, L. P., Fulton, R. E., and Suresh, M. R. (2001) *Biomol. Eng.* **18,** 31–40
6. Perisic, O., Webb, P. A., Holliger, P., Winter, G., and Williams, R. L. (1994) *Structure* **2,** 1217–1226
7. Arndt, M. A., Krauss, J., Kipriyanov, S. M., Pfreundschuh, M., and Little, M. (1999) *Blood* **94,** 2562–2568
8. Gao, Y., Xiong, D., Yang, M., Liu, H., Peng, H., Shao, X., Xu, Y., Xu, C., Fan, D., Qin, L., Yang, C., and Zhu, Z. (2004) *Leukemia* **18,** 513–520
9. Kipriyanov, S. M., Cochlovius, B., Schäfer, H. J., Moldenhauer, G., Bähre, A., Le Gall, F., Knackmuss, S., and Little, M. (2002) *J. Immunol.* **169,** 137–144
10. Xiong, D., Xu, Y., Liu, H., Peng, H., Shao, X., Lai, Z., Fan, D., Yang, M., Han, J., Xie, Y., Yang, C., and Zhu, Z. (2002) *Cancer Lett.* **177,** 29–39
11. Asano, R., Takemura, S., Tsumoto, K., Sakurai, N., Teramae, A., Ebara, S., Katayose, Y., Shinoda, M., Suzuki, M., Imai, K., Matsuno, S., Kudo, T., and Kumagai, I. (2000) *J. Biochem.* **127,** 673–679
12. Asano, R., Kudo, T., Nishimura, Y., Makabe, K., Hayashi, H., Suzuki, M., Tsumoto, K., and Kumagai, I. (2002) *J. Biochem.* **132,** 903–909
13. Asano, R., Sone, Y., Makabe, K., Tsumoto, K., Hayashi, H., Katayose, Y., Unno, M., Kudo, T., and Kumagai, I. (2006) *Clin. Cancer Res.* **12,** 4036–4042
14. Asano, R., Sone, Y., Ikoma, K., Hayashi, H., Nakanishi, T., Umetsu, M., Katayose, Y., Unno, M., Kudo, T., and Kumagai, I. (2008) *Protein Eng. Des. Sel.* **21,** 597–603
15. Le Gall, F., Reusch, U., Little, M., and Kipriyanov, S. M. (2004) *Protein Eng. Des. Sel.* **17,** 357–366
16. Kipriyanov, S. M., Moldenhauer, G., Braunagel, M., Reusch, U., Cochlovius, B., Le Gall, F., Kouprianova, O. A., Von der Lieth, C. W., and Little, M. (2003) *J. Mol. Biol.* **330,** 99–111
17. Pei, X. Y., Holliger, P., Murzin, A. G., and Williams, R. L. (1997) *Proc. Natl. Acad. Sci. U.S.A.* **94,** 9637–9642
18. Dolezal, O., Pearce, L. A., Lawrence, L. J., McCoy, A. J., Hudson, P. J., and Kortt, A. A. (2000) *Protein Eng.* **13,** 565–574
19. Power, B. E., Doughty, L., Shapira, D. R., Burns, J. E., Bayly, A. M., Caine, J. M., Liu, Z., Scott, A. M., Hudson, P. J., and Kortt, A. A. (2003) *Protein Sci.* **12,** 734–747
20. Le Gall, F., Reusch, U., Moldenhauer, G., Little, M., and Kipriyanov, S. M. (2004) *J. Immunol. Methods* **285,** 111–127
21. Hudson, P. J., and Kortt, A. A. (1999) *J. Immunol. Methods* **231,** 177–189
22. Wu, A. M., Chen, W., Raubitschek, A., Williams, L. E., Neumaier, M., Fischer, R., Hu, S. Z., Odom-Maryon, T., Wong, J. Y., and Shively, J. E. (1996) *Immunotechnology* **2,** 21–36
23. Adams, G. P., and Schier, R. (1999) *J. Immunol. Methods* **231,** 249–260
24. Blanco, B., Holliger, P., Vile, R. G., and Alvarez-Vallina, L. (2003) *J. Immunol.* **171,** 1070–1077
25. Bühler, P., Wolf, P., Gierschner, D., Schaber, I., Katzenwadel, A., Schultze-Seemann, W., Wetterauer, U., Tacke, M., Swamy, M., Schamel, W. W., and Elsässer-Beile, U. (2008) *Cancer Immunol. Immunother.* **57,** 43–52
26. Asano, R., Kawaguchi, H., Watanabe, Y., Nakanishi, T., Umetsu, M., Hayashi, H., Katayose, Y., Unno, M., Kudo, T., and Kumagai, I. (2008) *J. Immunother.* **31,** 752–761
27. Asano, R., Ikoma, K., Kawaguchi, H., Ishiyama, Y., Nakanishi, T., Umetsu, M., Hayashi, H., Katayose, Y., Unno, M., Kudo, T., and Kumagai, I. (2010) *FEBS J.* **277,** 477–487
28. Asano, R., Watanabe, Y., Kawaguchi, H., Fukazawa, H., Nakanishi, T., Umetsu, M., Hayashi, H., Katayose, Y., Unno, M., Kudo, T., and Kumagai, I. (2007) *J. Biol. Chem.* **282,** 27659–27665
29. Wiseman, T., Williston, S., Brandts, J. F., and Lin, L. N. (1989) *Anal. Biochem.* **179,** 131–137
30. Makabe, K., Nakanishi, T., Tsumoto, K., Tanaka, Y., Kondo, H., Umetsu, M., Sone, Y., Asano, R., and Kumagai, I. (2008) *J. Biol. Chem.* **283,** 1156–1166
31. Kjer-Nielsen, L., Dunstone, M. A., Kostenko, L., Ely, L. K., Beddoe, T., Mifsud, N. A., Purcell, A. W., Brooks, A. G., McCluskey, J., and Rossjohn, J. (2004) *Proc. Natl. Acad. Sci. U.S.A.* **101,** 7675–7680
32. Cochlovius, B., Kipriyanov, S. M., Stassar, M. J., Schuhmacher, J., Benner, A., Moldenhauer, G., and Little, M. (2000) *Cancer Res.* **60,** 4336–4341
33. Kipriyanov, S. M., Moldenhauer, G., Schuhmacher, J., Cochlovius, B., Von der Lieth, C. W., Matys, E. R., and Little, M. (1999) *J. Mol. Biol.* **293,** 41–56
34. Völkel, T., Korn, T., Bach, M., Müller, R., and Kontermann, R. E. (2001) *Protein Eng.* **14,** 815–823
35. Kortt, A. A., Dolezal, O., Power, B. E., and Hudson, P. J. (2001) *Biomol. Eng.* **18,** 95–108
36. Schlereth, B., Fichtner, I., Lorenczewski, G., Kleindienst, P., Brischwein, K., da Silva, A., Kufer, P., Lutterbuese, R., Junghahn, I., Kasimir-Bauer, S., Wimberger, P., Kimmig, R., and Baeuerle, P. A. (2005) *Cancer Res.* **65,** 2882–2889
37. Shahied, L. S., Tang, Y., Alpaugh, R. K., Somer, R., Greenspon, D., and Weiner, L. M. (2004) *J. Biol. Chem.* **279,** 53907–53914
38. Ravn, P., Danielczyk, A., Jensen, K. B., Kristensen, P., Christensen, P. A., Larsen, M., Karsten, U., and Goletz, S. (2004) *J. Mol. Biol.* **343,** 985–996
39. Dolezal, O., De Gori, R., Walter, M., Doughty, L., Hattarki, M., Hudson, P. J., and Kortt, A. A. (2003) *Protein Eng.* **16,** 47–56

the FEBS Journal

Application of the Fc fusion format to generate tag-free bi-specific diabodies

Ryutaro Asano[1], Keiko Ikoma[1], Hiroko Kawaguchi[1], Yuna Ishiyama[1], Takeshi Nakanishi[1], Mitsuo Umetsu[1], Hiroki Hayashi[2], Yu Katayose[2], Michiaki Unno[2], Toshio Kudo[3] and Izumi Kumagai[1]

1 Department of Biomolecular Engineering, Graduate School of Engineering, Tohoku University, Sendai, Japan
2 Division of Gastroenterological Surgery, Department of Surgery, Graduate School of Medicine, Tohoku University, Sendai, Japan
3 Cell Resource Center for Biomedical Research, Institute of Development, Aging and Cancer, Tohoku University, Sendai, Japan

Keywords
bi-specific diabody; Fc fusion format; preparation method; small therapeutic antibody; tag-free protein

Correspondence
I. Kumagai, Aoba 6-6-11-606, Aramaki, Aoba-ku, Sendai 980-8579, Japan
Fax: +81 22 795 6164
Tel: +81 22 795 7274
E-mail: kmiz@kuma.che.tohoku.ac.jp

(Received 1 May 2009, revised 9 November 2009, accepted 17 November 2009)

doi:10.1111/j.1742-4658.2009.07499.x

We previously reported the use of a humanized bi-specific diabody that targets epidermal growth factor receptor and CD3 (hEx3-Db) for cancer immunotherapy. Bacterial expression can be used to express small recombinant antibodies on a large scale; however, their overexpression often results in the formation of insoluble aggregates, and in most cases artificial affinity peptide tags need to be fused to the antibodies for purification by affinity chromatography. Here, we propose a novel method for preparing refined, functional, tag-free bi-specific diabodies from IgG-like bi-specific antibodies (BsAbs) in a mammalian expression system. We created an IgG-like BsAb in which bi-specific diabodies were fused to the human Fc region via a designed human rhinovirus 3C (HRV3C) protease recognition site. The BsAb was purified by protein A affinity chromatography, and the refined tag-free hEx3-Db was efficiently produced from the Fc fusion format by protease digestion. The tag-free hEx3-Db from the Fc fusion format showed a greater inhibition of cancer growth than affinity-tagged hEx3-Db prepared directly from Chinese hamster ovary cells. We also applied our novel method to another small recombinant antibody fragment, hEx3 single-chain diabody (hEx3-scDb), and demonstrated the versatility and advantages of our proposed method compared with papain digestion of hEx3-scDb. This approach may be used for industrial-scale production of functional tag-free small therapeutic antibodies.

Introduction

Bi-specific antibodies (BsAbs) are attractive formats for recombinant antibodies that can bind to two different epitopes on antigens. This bi-specificity can be used in cancer immunotherapy by cross-linking tumor cells to immune cells such as cytotoxic T cells, natural killer cells and macrophages. This linkage accelerates the destruction of the tumor cells by immune cells, so that the dose of therapeutic antibodies can be reduced from that required in the case of mono-specific antibodies [1,2].

Abbreviations
BsAbs, bi-specific antibodies; CHO, Chinese hamster ovary; Db, diabody; EGFR, epidermal growth factor receptor; hEx3-Db, humanized bi-specific diabody that targets epidermal growth factor receptor and CD3; hEx3-scDb, hEx3 single-chain diabody; HRV3C, human rhinovirus 3C; MTS, 3-(4,5-dimethylthiazole-2-yl)-5-(3-carboxymethoxyphenyl)-2-(4-sulfophenyl)-2*H*-tetrazolium inner salt; scDb, single-chain diabody; scFv, single chain Fv; T-LAK, lymphokine-activated killer cells with the T-cell phenotype; tanDb, tandem single-chain diabody; taFv, tandem scFv.

Conventionally, BsAbs are produced by chemical conjugation or somatic fusion of two hybridomas, forming a quadroma that can produce bi-specific IgG molecules [1,3]. Clinical studies of these BsAbs have been performed, and some impressive local anti-tumor responses have been reported; however, these trials have also been limited by the occurrence of human anti-mouse antibody and/or Fc-mediated side-effects such as the induction of a cytokine storm [4,5]. Furthermore, these methods cannot be utilized for large-scale production, and a quadroma cannot control the heterogeneity of the antibodies produced; for instance, ten possible variants of antibodies can be generated when two heavy and two light chains are randomly associated. Therefore, steady production of homogeneous BsAbs requires the use of a host-vector system.

Advances in antibody engineering techniques and host-vector expression systems have facilitated the generation of recombinant BsAbs with improved properties. A variety of recombinant BsAbs have been developed from two antibody fragments such as single-chain Fv fragments (scFv; 25 kDa) [6,7], and diabodies (Db; 55 kDa) [8] that recognize different antigens. The most common BsAb formats that have been produced from these fragments are tandem scFv (taFv) [9], tandem single-chain diabodies (tandem scDb, tanDb) [10] and mini-bodies (dimeric scDb–CH3 fusion protein) [11]. Compared with classic BsAbs prepared by chemical conjugation or production of a quadroma, small antibody molecules, such as diabodies, are of a suitable size for rapid tissue penetration, high target retention and rapid clearance [12,13]. Their smaller size also enables expression of BsAbs in bacteria, and as the structure is composed only of antibody variable regions, this eliminates the Fc-mediated side-effects of BsAbs. Although the rapid blood clearance and monovalency of bi-specific diabodies, scDbs and taFv (all approximately 55 kDa) may limit their therapeutic application, engineering the length and amino acid composition of the middle linker in scDb, for example, may enable them to assemble into multimers, such as tanDb (114 kDa), with higher molecular weight and bivalency for each target antigen [14,15].

Small bi-specific antibody fragments prepared in bacteria are often expressed as insoluble aggregates in the cytoplasmic or periplasmic space [10,16–18], and require fusion of artificial affinity peptide tags, such as a polyhistidine tag, hemagglutinin tag or FLAG tag, at the N- or C-terminus of the BsAbs to allow complete removal of the vast amount of host-derived proteins by affinity chromatography [16,19]. The requirement for such tags raises concerns about immunogenicity. We have previously reported significant anti-tumor activity *in vitro* and *in vivo* for a humanized bi-specific diabody targeting epidermal growth factor receptor (EGFR) and CD3 (hEx3-Db) [20]. However, even though the yield of hEx3-Db was over 10 $mg \cdot L^{-1}$ culture, it was also expressed as insoluble aggregates, and fusion of an affinity tag was necessary for purification before the re-folding process.

We have also reported the construction of a mammalian expression system for affinity-tagged bi-specific diabodies and their Fc fusion formats [21]. Here, we developed a novel method for the production of highly purified tag-free diabodies using the mammalian expression system. Diagrams of the various gene constructs are shown in Fig. 1. The tag-free hEx3-Db alone was expressed sufficiently to be purified by ion-exchange chromatography. Expression of the hEx3 diabodies fused to the human Fc region via a designed protease recognition site enabled high-efficiency purification by protein A affinity chromatography and increased the yield of tag-free hEx3-Db. We also used our method to produce tag-free small BsAbs to hEx3-scDb. For hEx3-scDb, use of the designed protease recognition site had advantages over papain digestion, which caused unwanted degradation. Both tag-free hEx3-Db and hEx3-scDb prepared by restriction protease digestion from the Fc fusion format showed a greater inhibition of cancer growth *in vitro* than previously produced affinity-tagged diabodies directly prepared from the supernatant of Chinese hamster ovary (CHO) transfectants [21]. Thus, this approach appears to improve both the yield and efficacy of the bi-specific antibody fragments.

Results

Preparation of tag-free bi-specific diabodies

Tag-free hEx3-Db was directly secreted from mammalian cells and purified by cation-exchange chromatography as described in Experimental procedures. Purified hEx3-Db was applied to a gel filtration column for further analysis and purification (Fig. 2A). The first small peak, second large peak and the shoulder of the major peak seen in the chromatograph were identified as the multimeric, dimeric and monomeric structures of tag-free hEx3-Db, respectively. Equivalent amounts of hOHh5L (humanized OKT3 VH - linker - humanized 528 VL) and h5HhOL (humanized 528 VH - linker - humanized OKT3 VL) were confirmed in the dimeric fraction by SDS–PAGE analysis (Fig. 2B). Thus, purified tag-free hEx3-Dbs were obtained without affinity chromatography at a final yield of approximately 1 $mg \cdot L^{-1}$ culture.

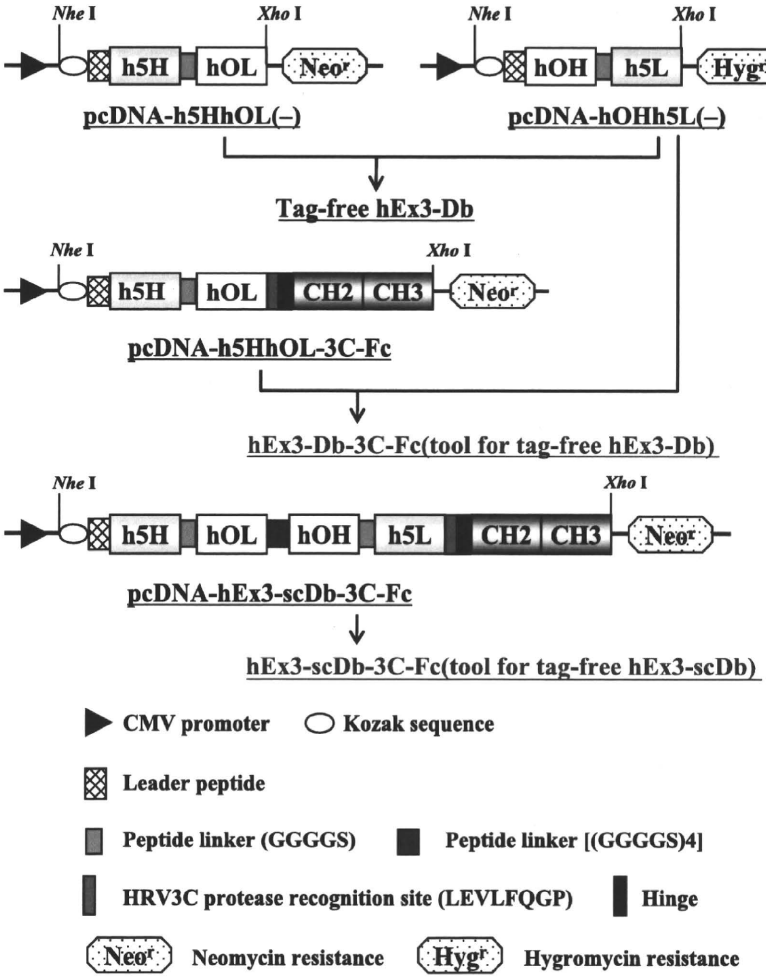

Fig. 1. Schematic illustration of the BsAb gene constructs in pCDNA3.1. The V^H and V^L regions of humanized 528 Fv are designated h5H and h5L, and those of humanized OKT3 Fv are designated hOH and hOL, respectively. The positions of important restriction enzyme sites used and the key components are shown.

To prepare the high-quality, tag-free bi-specific diabodies, we fused the hEx3-Db to the human IgG1 Fc region. We inserted a recognition site for HRV3C protease between the diabody fragments and the Fc portion of hEx3-Fc. A schematic illustration of the preparation of tag-free hEx3-Db from its Fc fusion format is shown in Fig. 3A. The expressed IgG-like BsAbs were purified by protein A affinity chromatography and digested using glutathione *S*-transferase (GST)-fused HRV3C protease. The treated solution was loaded onto a glutathione-immobilized column and then a protein A column to remove added protease and digested Fc. SDS–PAGE analysis of each purification step showed the successful preparation of tag-free hEx3-Db from its Fc fusion format (Fig. 3B). Gel filtration chromatography showed that tag-free hEx3-Db predominantly formed dimers, with a small amount of multimeric forms (Fig. 4A). The homogeneity of tag-free hEx3-Db in the eluted fraction was also confirmed by SDS–PAGE (Fig. 4B). The final yield of tag-free hEx3-Db from the Fc fusion format was approximately 5 $mg \cdot L^{-1}$ culture, i.e. five times that of the secreted tag-free hEx3-Db. Thus, secretion of BsAbs as the Fc fusion format increased the amount of prepared tag-free diabodies due to the high productivity (approximately 10 $mg \cdot L^{-1}$) and the efficient purification using protein A.

Mass spectrometry of tag-free bi-specific diabodies

We previously reported that the strong inter-domain interaction between cognate V^H and V^L domains of hEx3-Db leads to the spontaneous formation of functional heterodimers [22]. In the present study, the molecular weight of the monomorphous heterodimer of the tag-free hEx3-Db prepared from the Fc fusion format was confirmed by MALDI-TOF mass spectrometry (Fig. 4C). The mass spectrum for the diabodies prepared from the Fc fusion format had two peaks, one at *m/z* 26 424 and another at *m/z* 25 970, which correspond to the calculated molecular weights of

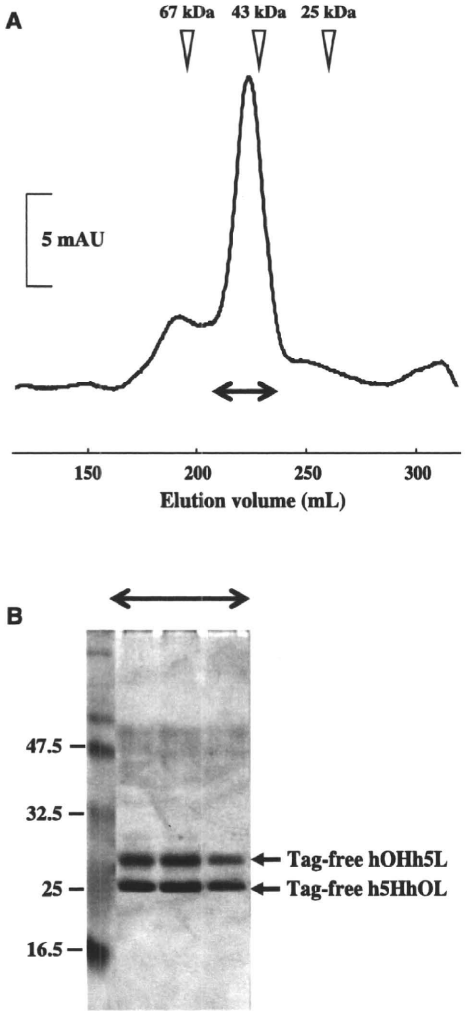

Fig. 2. (A) Gel filtration of tag-free hEx3-Db. The elution volume is shown on the *x* axis, and the molecular mass (kDa) is shown above. The eluted fractions containing the bi-specific diabody are indicated by the two-headed arrow. (B) SDS–PAGE analysis under reducing conditions of the eluted fraction. Molecular size markers are shown on the left.

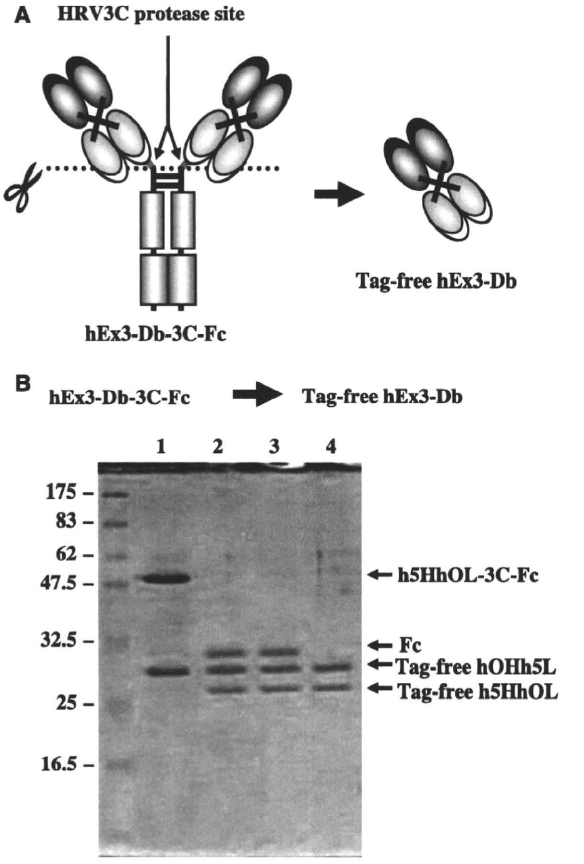

Fig. 3. (A) Schematic illustration of the hEx3-Db–3C–Fc fusion protein. The HRV3C protease cleavage site used for preparation of tag-free hEx3-Db is indicated. (B) Reducing SDS–PAGE of each purification step for preparation of tag-free hEx3-Db from hEx3-Db–3C–Fc. Lane 1, protein A chromatography-purified hEx3-Db–3C–Fc; lane 2, after HRV3C protease digestion; lane 3, after removal of HRV3C protease by glutathione Sepharose 4B chromatography; lane 4, purified tag-free hEx3-Db after removal of the Fc region by protein A chromatography.

hOHh5L digested from the Fc fusion (26 442) and h5HhOL without the peptide tag (25 991), respectively. These results indicate that Db–3C–Fc fusion proteins can serve as a tool for preparing tag-free diabodies with high yield and purity.

Binding affinity of tag-free bi-specific diabodies and its effect on growth inhibition

The binding affinity of tag-free hEx3-Dbs for CD3-positive lymphokine-activated killer cells with the T-cell phenotype (T-LAK cells) and EGFR-positive TFK-1 cells was measured by flow cytometry using polyclonal antibody to hEx3-Db. Tag-free hEx3-Dbs interacted with each targeted antigen (Fig. 5A), and the binding profiles were comparable with those previously reported for affinity-tagged hEx3-Db [20,22]. These results indicate that the diabody prepared by HRV3C protease digestion from the Fc fusion format retained sufficient binding activity and bi-specificity.

To evaluate the inhibition of cancer growth by tag-free hEx3-Db, an MTS assay was performed for TFK-1 cells by using T-LAK cells at an effector/target ratio of 5 : 1. Tag-free hEx3-Db prepared from the Fc fusion format inhibited cancer cell growth more effectively than did affinity-tagged hEx3-Db (Fig. 5B). Imperceptible differences in purity and local structural perturbations that are dependent on the preparation method might affect these activities.